Reflections on the effect of an external flux in surface physics

Stefano Curiotto, F. Leroy, F. Cheynis, P. Müller

this is a preprint, the final version is published in:
Surface Science 725 (2022) 122158
https://doi.org/10.1016/j.susc.2022.122158

Reflections on the effect of an external flux in surface physics

S. Curiotto, F. Leroy, F. Cheynis, P. Müller

Aix Marseille Univ, CNRS, CINaM, AMUTECH, Marseille, France

Abstract

Sublimating surfaces are out of equilibrium. It has been proposed that sublimation can be compensated by an impinging atomic flux to obtain equilibrium. This work concerns the effect of such an impinging flux on the stability of surfaces in various situations. For this purpose we combine Kinetic Monte Carlo Simulations with analytical developements based on the Burton-Cabrera-Frank (BCF) classical theory. We show that a perfect compensation of the sublimation is possible for vicinal surfaces but not when 2D islands are present on a surface. We thus study the effect of an impinging flux on the dynamic of a 2D island on a surface. We show that the 2D island area generally varies with time t as $-t^{\alpha}$. In absence of any impinging flux the value of the exponent α enables to identify the main mechanism at work (diffusion limited or attachment-detachment limited). On the contrary, in presence of an impinging flux the value of the exponent α is not enough to identify the main mechanism limiting the area change.

1. Introduction

Crystal growth and sublimation experimental studies respectively require a complete control of the supersaturation or undersaturation conditions. From an historical point of view, most of the first surface science experiments have been performed in Ultra High Vacuum conditions that means without any control of the super or undersaturation conditions.
At the end of the sixties, Bethge et al. [1–3] proposed a simple method to control super(under)saturation conditions in a microscope. This method has been systematically used by J.J. Metois and coworkers [4–7] for studying silicon growth and silicon sublimation in a Reflection Electron Microscope (REM). The method consisted in mounting face-to-face in the same sample-holder two silicon wafers (called the substrate and the source) that can be heated independently at two different temperatures T_{source} and T_{sample} high enough to ensure Si sublimation. In such experimental conditions two fluxes exist on the substrate: the desorbing flux J_{des} (due to the substrate sublimation) and the impinging flux J_{im} (due to the source sublimation). If $J_{des} > J_{im}$ the substrate sublimates, if $J_{im} > J_{des}$ the substrate grows and if $J_{im} = J_{des}$ a steady state is expected. For a simple vicinal substrate, the monoatomic steps thus recede in sublimation conditions ($J_{des} > J_{im}$) or advance in growth conditions ($J_{im} > J_{des}$) but fluctuate on the spot and thus do not displace in steady conditions ($J_{im} = J_{des}$). Such an impinging flux has thus been used to balance the sublimation for studying step fluctuations at equilibrium [4–7]. In the semiconductor industry, wafers are often annealed in stacks where the flux of atoms sublimating from a wafer constitutes an impinging flux for nearby wafers. Therefore the compensation of sublimation is also important in applications [8].

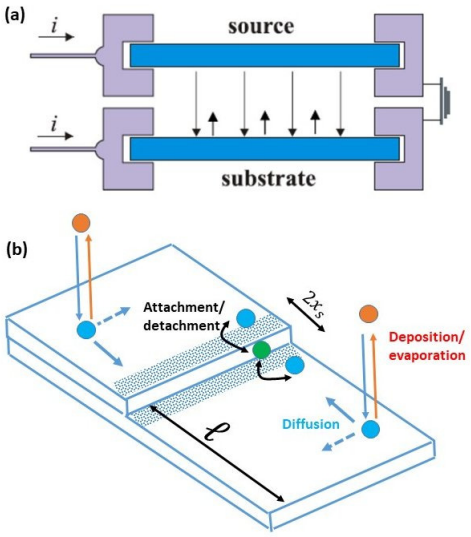

Figure 1: *(a) Experimental system used to compensate the sample (substrate) sublimation by an impinging flux originating from a second sample (source). (b) Sketch of atomic exchanges on a surface formed by two terraces of width ℓ separated by a monoatomic step (height a). The width $2x_s$ corresponds to the capture zone.*

In this paper we discuss the conditions for a possible compensation of sublimation. We will start describing vicinal surfaces. We will show that, if a balance between sublimation and an additional impinging flux can be reached for a vicinal surface, it is not the case for 2D islands on a surface. In this last case we will discuss the effect of sublimation and deposition on the dynamical evolution of a 2D-island. For this purpose we will combine KMC simulations with analytical models.

2. Simple case of a vicinal surface

A flat surface in equilibrium with a saturated vapour exhibits an adsorbed layer characterized by a constant adatom density $n(x) = n_{eq}$ maintained by atomic exchanges with the saturated vapour. A vicinal surface at equilibrium is also characterized by a constant adatom density, however if far from the steps the equilibrium density n_{eq} is still maintained by atomic exchanges with the saturated vapour, at the steps the atomic exchanges essentially take place between the steps and the adsorption layer so that direct exchanges with the vapor can be neglected at the steps (see Figure 1b).

In out-of-equilibrium conditions (growth or sublimation), the classical BCF description [9] assumes that a positive (growth) or negative (sublimation) flux does not perturbate the equilibrium density at the steps. The step velocity is thus directly proportionnal to the supersaturation $J_{in} - J_{des}$.

We use Kinetic Monte Carlo simulations to study the sublimation of a vicinal surface (for details on the methodology see appendix I) formed by monoatomic steps separated by flat terraces of width ℓ as shown in Figure 1b.

Figure 2a shows that the sublimation rate of the vicinal surface depends on the step density that means on its vicinality. The black squares in Figure 2b show the total number of atoms versus time in pure sublimation regime for a surface with two terraces separated by an atomic step. The sublimation rate is obtained from the slope of the linear fit through the data. The red dots in Figure 2b refer to a simulation performed with an additional impinging flux equal to the sublimation flux found in the pure sublimation regime. Contrary to what a naive view would suggest, in spite of the supposedly perfect compensation, the number of adatoms still decreases with time. In other words an impinging flux equal to the sublimation flux is not enough to compensate the sublimation. Actually a true compensation (that means a constant number of atoms) is only reached when the sublimating flux is overcompensated (blue triangles). The empty green triangles in Figure 2b refer to a surface with a step density twice that of the previous surface (black squares) having thus a higher sublimation rate. However, less intuitively at a first sight, the total impinging flux necessary to exactly compensate the sublimation (that means impinging flux equal to the sublimation flux + overcompensation) is the same for the two surfaces. More generally, this compensation flux does not depend on the step density (or the vicinality angle).

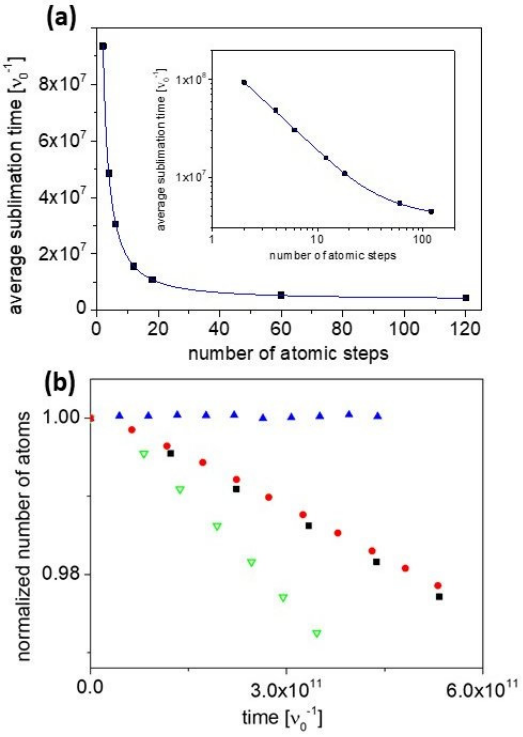

Figure 2: *(a): Average time between the sublimation of two atoms (black squares) obtained by KMC versus the vicinality measured by the number of steps for a simulation box with 600x600 atomic positions (k_BT=0.25, E_{ev} = 1) The continuous line corresponds to a fit from equation 2 with $J_{in} = 0$, (b) Normalized number of atoms on the surface for a surface with 2 terraces (black squares). This number decreases due to the sublimation. When the sublimation flux is balanced by an impinging flux (red points) corresponding to the evaporation flux measured for the black squares (id-est 1 atom every $9\,10^7\,\nu_o^{-1}$) the supposed compensation does not allow to reach a constant number of atoms on the surface. An overcompensatig flux is necesssary (blue triangles, 1 atom deposited every $4\,10^6\,\nu_o^{-1}$). A surface with 4 steps (green triangles) sublimates more but the total flux (impinging flux equal to the sublimating flux+ overcompensation) necessary to reach a constant number of atoms on the surface is the same as that found with two steps (blue triangles).*

All these results may be understood within the classical BCF model [9] which states that the change of the adatom density n(x) at a location x on the surface is described by the diffusion equation:

$$\frac{dn}{dt} = J_{in} + D\nabla^2 n - \frac{n}{\tau} \qquad (1)$$

where J_{im} is the impinging external flux, $D\nabla^2 n$ the diffusing surface flux induced by the concentration gradient (D being the surface diffusion constant) and $J_{des} = n/\tau$ the desorption flux with τ the mean adatom sublimation time.

In the stationary state $\left(\frac{dn}{dt} = 0\right)$, the solution reads $n(x) = J_{im}\tau + Ae^{x/x_s} + Be^{-x/x_s}$ where $x_s = \sqrt{D\tau}$ is the mean length of surface diffusion. Thus a region of width $2x_s$ centered on a step corresponds to a "capture zone" where the probability of adatoms to be captured by the step is higher than the sublimation probability (see Figure 1b). The constants A and B are determined by boundary conditions that describe the

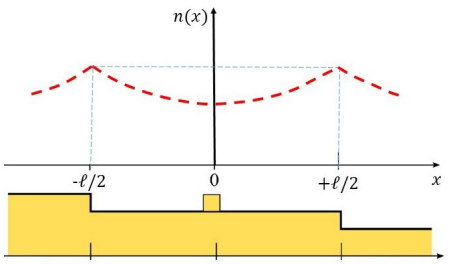

Figure 3: *Classical BCF description of the adatom density on a terrace between two steps in the sublimation regime.*

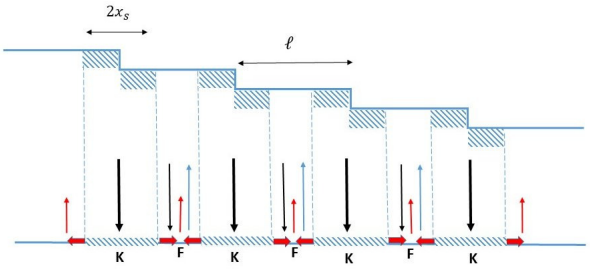

Figure 4: *Illustration of equation 3. In the diffusion limited regime, a stepped (S) surface (top) is equivalent to an alternance of kinked (K) and flat (F) areas (bottom) [11]. Adatoms trapped by the K zones may detach and diffuse on the F zone (horizontal red arrows) before desorbing (vertical red arrows) whereas atoms landing on F parts because of the impinging flux (black arrows) directly desorb after a mean time τ (blue arrows). The desorbing flux thus has two contributions (red and blue arrows) the ratio of which depends on ℓ/x_s that means, for a given value of x_s, on the vicinality angle θ given by $\tan\theta = a/\ell$ where a is the atomic height of a step.*

relationship between the flux towards the steps framing a terrace and the rate of incorporation at these step-edges. They read $D\frac{dn}{dx} = \pm\kappa(n - n_{eq})$ at the step positions $\pm\ell/2$ with n_{eq} the equilibrium adatom density and κ a kinetic coefficient for adatom attachment/detachment at the steps (see Figure 3 where is reported $n(x)$ in the pure sublimation regime). We thus find $A = B = (J_{im} - n_{eq}/\tau)\left[\left(1 - \frac{d}{x_s}\right)e^{-\ell/2x_s} + \left(1 + \frac{d}{x_s}\right)e^{\ell/2x_s}\right]^{-1}$.

The new characteristic kinetic length $d = D/\kappa$ roughly corresponds to the mean length an adatom runs along a step before being incorporated into it [10]. The step velocity corresponds to the net flux of adatoms reaching the step (horizontal blue arrows in Figure 1b) , that means

$$V = a^2 D\left[\left.\frac{dn}{dx}\right]_{-\ell/2} - \left.\frac{dn}{dx}\right]_{+\ell/2}\right]$$

(a^2 being an atomic area), and thus:

$$V = 2a^2 x_s\left(J_{im} - \frac{n_{eq}}{\tau}\right)\frac{2\sinh\left(\ell/2x_s\right)}{\left(1 - \frac{d}{x_s}\right)e^{-\ell/2x_s} + \left(1 + \frac{d}{x_s}\right)e^{\ell/2x_s}} \quad (2)$$

For instantaneous adatom incorporation, also called diffusion-limited regime, ($D << \kappa$ or $d \to 0$) the usual classical BCF result is recovered:

$$V_0 = 2a^2 x_s\left(J_{im} - \frac{n_{eq}}{\tau}\right)\tanh\left(\frac{\ell}{2x_s}\right) \quad (3)$$

When $\ell << 2x_s$ this last expression gives $V_0 = a^2\ell\left(J_{im} - \frac{n_{eq}}{\tau}\right)$ that means that all the adatoms landing on a given terrace of size ℓ are incorporated in the steps whereas when $\ell >> 2x_s$ there is $V_0 = 2a^2 x_s\left(J_{im} - \frac{n_{eq}}{\tau}\right)$ that means that only the adatoms landing within a capture zone of witdth $2x_s$ are incorporated. In the general case $\ell > 2x_s$, we can describe a vicinal surface in the diffusion limited regime as a successive alternance of Kinked (K) zones (where landing adatoms are trapped) and of Flat (F) zones (where landing adatoms sublimate), see Figure 4.

For pure sublimation the steps recede with a velocity V_{ev} obtained by putting $J_{im} = 0$ in equation 2. We can extract a mean time for adatom desorption $< t_{des} >= \frac{a^2}{V_{ev}NL}$ where a^2 is an atomic area, L the step length and N the number of steps in the simulation box. The sublimation flux thus depends on the vicinality. The analytical expression of $< t_{des} >$ perfectly fits the vicinality dependence deduced from KMC (with d as a fitting parameter [1]) in Figure 2a . However since $\left(J_{im} - \frac{n_{eq}}{\tau}\right)$ is a prefactor in equation 2 the true impinging flux necessary to reach the steady state $V = 0$ is still $J_{im} = \frac{n_{eq}}{\tau}$ and thus does not depend on the vicinality, as found in the KMC simulations [2]. Because of the vicinality factor $\frac{2\sinh(\ell/2x_s)}{\left(1-\frac{d}{x_s}\right)e^{-\ell/2x_s}+\left(1+\frac{d}{x_s}\right)e^{\ell/2x_s}}$ smaller than unity that appears in the expression 2 of V_{ev}, the sublimation rate depends on the interstep distance and is smaller than $\frac{n_{eq}}{\tau}$. This explains why an overcompensation of the sublimation is necessary in KMC simulations.

3. Case of 2D islands

In the following we reconsider the evolution of a 2D island on a surface with the two main underlying questions: (i) What is the dynamical evolution of a 2D-island in presence of both sublimation and external fluxes ? (ii) Is it possible to compensate the desorption ? For this purpose we will consider three configurations (see Figure 5): a 2D island on a terrace framed by two steps, a 2D island in a hole, and a 2D island on top of another, larger, 2D island (wedding cake configuration).

[1] We take n_{eq} corresponding to the simulated equilibrium concentration found by counting the number of atoms on the surface without sublimation.

[2] Directly solving equation 1 with $J_{in} = n/\tau$ and $dn/dt = 0$ leads to $n = n_{eq}$ constant on the whole surface.

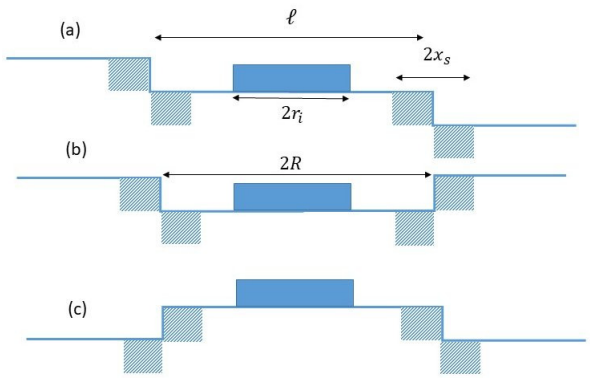

Figure 5: *Studied configurations of a 2D island (radius r_i) on : (a) a terrace framed by two steps, (b) a hole (radius R), (c) on top of another 2D island (radius R). This last case is also called wedding cake configuration. The cross-hatched zones schematize the capture zones of width $2x_s$ around steps.*

3.1. Dynamical evolution of a 2D-island in presence of sublimation and external flux

The stability and the dynamical evolution of 2D nanostructures have been studied in many different works. Among them the case of a single 2D island on a surface has received an increasing interest [12–19]. Indeed, the kinetics of growth or decay of a 2D island may give information on the relative importance of surface diffusion and attachment/detachment mechanisms at step edges. More precisely, at low temperature (no sublimation and no external flux) the islands simply shrink because of the Gibbs-Thomson effect [20, 21], which states that the chemical potential of a nano-object increases when its size decreases. The area of a 2D circular island is often considered to change with time according to a scaling law $A(t) \propto (t_0 - t)^{\alpha}$ where the exponent α varies in a complex way. However two limiting cases have been described: $\alpha \to 2/3$ for diffusion limited regime but $\alpha \to 1$ for attachment/detachment limited regime [12–16]. J.J. Metois et al. used the experimental configurations of Figure 1 and assumed that the impinging flux compensates sublimation [4, 6, 22].

This section is thus devoted to a complete study of the behaviour of a 2D island in presence of sublimation (as done by Altman and coworkers [16, 23]) but with an additional external impinging flux. The main question is: is it still possible to describe the dynamics of island shrinking by universal scaling laws $A(t) \propto (t_0 - t)^{\alpha}$ with an exponent α that, at least in a few limiting cases, simply depends on the mechanism at work (diffusion or attachment/detachment limited) ?

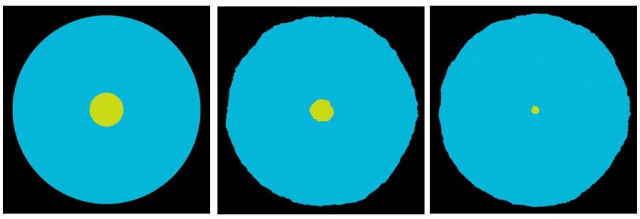

Figure 6: *Snapshots of KMC simulation of island decay in the wedding cake configuration. The inner island of radius $r_i = 46$ (yellow) ion a blue terrace of radius $R = 250$ disappears with time whatever the configuration (island in a hole or wedding cake configuration). ($k_BT = 0.25J$, simulation box 600x600). Notice that the step edges of both the inner and the outer islands fluctuate. These fluctuations are neglected in the analytical developments reported in the following.*

At first let us use KMC simulations to study the behaviour of an island of radius r_i in two configurations (i) in a hole of larger radius R, (ii) on top of another 2D island of radius R (wedding cake configuration). We find that the island area can be fitted by a power law $A(t) \propto (t_0 - t)^{\alpha}$ (see Figure 7a). However the value of the exponent α depends on the configuration and leads to a faster shortening for a island in a hole than for the wedding cake. The evolution of the exponent α versus the size of the external radius R is reported in figure 7b for a starting value r_i=45 for different configurations and temperatures. For large values of r_i/R, the distance between the edge of the island and that of the hole or of the lower island is small so that the diffusion distance is small and the 2D island shrinking is mainly limited by the time necessary to attach and detach atoms from the edges (see Figure 5). On the contrary, for small values of r_i/R, the mechanism is diffusion limited and α tends towards 2/3 as experimentally found by Leroy and coworkers for Si(111) [24]. Actually, the absolute value of R plays a role and not only the ratio r_i/R. If both values of r_i and R are small the island decay can be attachment/detachment limited.

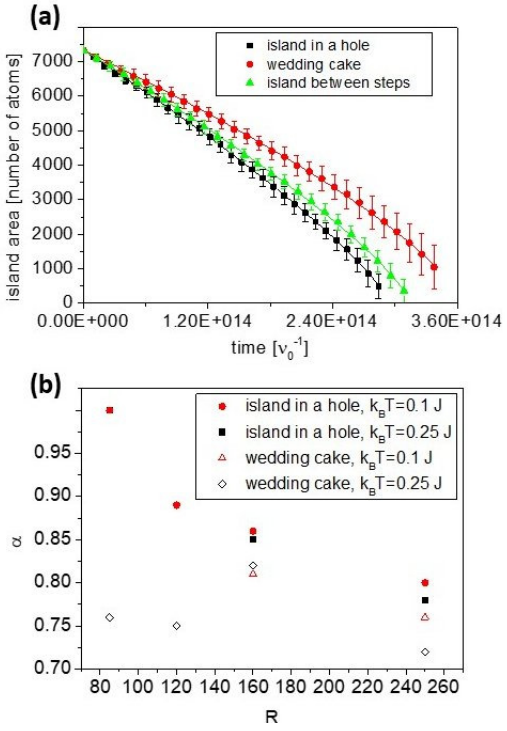

Figure 7: *(a) Fit of the island area $A(t) \propto (t_0 - t)^{\alpha}$ for three configurations: island in a hole (black squares), island between two steps (green triangles) and wedding cake configuration (red circles). (k_BT=0.25 J, r_i = 45, R = 250,Simulation box 600x600). (b) Evolution of the exponent α versus the radius R of the outer island for two temperature and two configurations (island in a hole and wedding configuration).*

Figure 8 shows the results of the KMC simulations for a 2D island in a hole in three cases: (a) limited by the diffusion, (b) limited by sublimation and (c) in presence of an impinging flux that exactly compensates the sublimation.

In our KMC simulations the additional impinging flux is implemented with the following procedure: every desorbed atom that leaves the surface is replaced by a new adatom deposited on the surface at a random position. In evaporation, since the number of atoms that leave the surface depends on the adatom concentration which depends on the island size (Gibbs-Thomson effect), the island shrinking leads to a desorbing flux that varies with time (see following section). Thus, in the KMC simulations of figures 8c and 9b, the additional impinging flux exactly compensates the desorbing flux. Thus it is not constant but varies with time. The best fit of the island area again scales as $A(t) \propto (t_0 - t)^{\alpha}$ with respectively $\alpha \approx 0.78$, $\alpha \approx 1.7$ and $\alpha \approx 0.99$ for the casesof Figures 8 a, b and c respectively. Figure 9a shows that the exponent α increases with temperature T for a given sublimation energy barrier.

Figure 9b shows the values of the exponent α for various sublimation energiy barriers (let us remind that the greater the sublimation energy is, the weaker the sublimation is). The black squares correspond to simulations without any external flux (only sublimation and surface diffusion), the exponent varies from $\alpha \approx 1.7$ for high sublimation rate (close to $\alpha = 2$ expected for pure sublimation) to weaker values $\rightarrow 0.7$ when sublimation vanishes (close to $\alpha = 2/3$ expected for pure diffusion). The red squares correspond to the same simulations in presence of a non constant external flux that exactly balances the desorbing flux. The exponent α now remains close to unity for high sublimation then again tends towards $\alpha \rightarrow 2/3$ when there is no more sublimation (and thus no more external flux). In other words the exponent, valid for pure diffusion, increases when increasing the supplemental impinging flux.

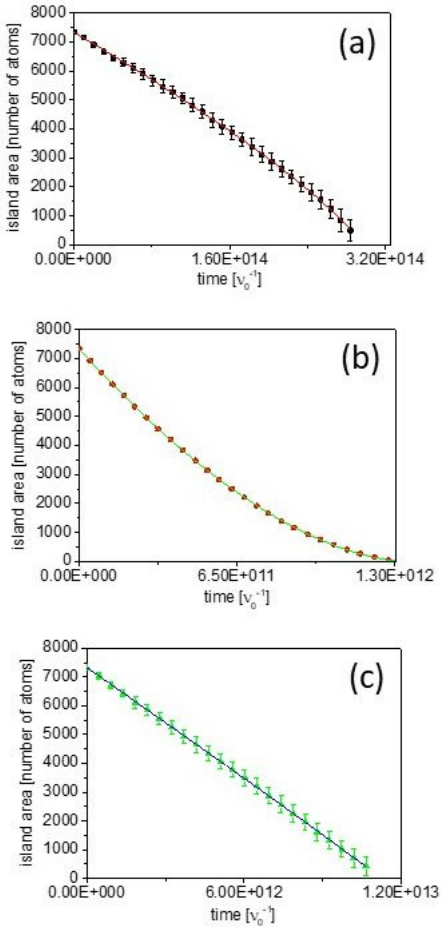

Figure 8: *Islanf area as a function of time simulated by KMC in different regimes: (a) Diffusion limited ($d \rightarrow 0$), the scaling law is $A(t) \propto t^{0.78}$ close to $t^{2/3}$ expected for pure diffusion, (b) sublimation limited ($x_s \rightarrow 0$), $A(t) \propto t^{1.72}$ close to t^2 expected for pure sublimation, (c) The impinging flux exactly compensates the sublimation, $A(t) \propto t^{0.9}$ close to t^1 (see table 1). (k_BT=0.25 J, R = 250, r_i = 45,Simulation box 600x600. For (b) the evaporation energy is 0.3 J).*

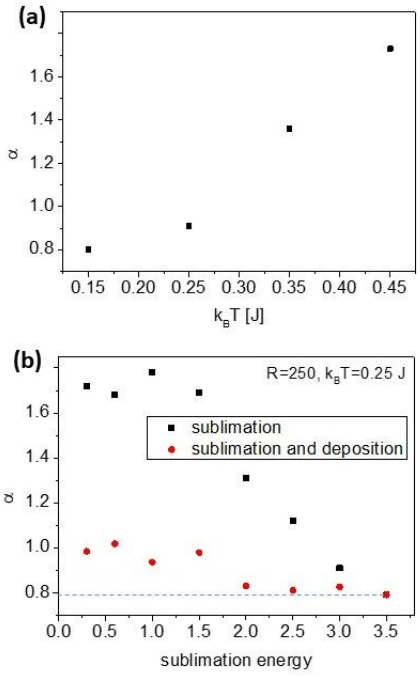

Figure 9: *Variation of the exponent α (a) with temperature for a given sublimation energy $E_{ev} = 3J$ (see appendix I), (b) with the sublimation energy for a given temperature. The reported results correspond to the configuration island in a hole and are similar to those of the wedding cake configuration. Let's notice that for $E_{ev} = 3.5$ there is no more sublimation so that the last red circle actually corresponds to the limit value of α without any sublimation nor deposition. ($R = 250$, $r_i = 45$,Simulation box 600x600).*

The behaviour of a 2D circular island with sublimation and impinging flux may be analytically studied on the basis of the BCF approach [9]. For the sake of clarity, all the analytical developments are reported in appendix II. They give access to an analytical expression of the variation dA/dt versus the island radius but cannot be directly integrated to get an explicit expression of $A(t)$. A few universal scaling laws of dA/dt and $A(r_i) = \pi r_i^2$ obtained as limiting cases of appendix II are reported in table 1.

The area variation $\frac{dA}{dt}$ of equation 14 of appendix II is a function of seven parameters n_{eq},D, r_i, R, x_s,$J_{in}\tau$, d. For the discussion we will fix the size of the external radius R as well as the values of n_{eq} and D. There remains three parameters: x_s, $J_{in}\tau$, d. For the discussion we will represent dA/dt versus r_i for d varying from the so-called diffusion limited case ($d \to 0$) to the so-called attachment/detachment case ($d \to \infty$). We will thus study the effect of sublimation (the smaller x_s is, the greater the sublimation is) with and without the presence of a flux J_{in}.

Limited	Assumptions	$\frac{dA}{dt} \propto$	$A(t) \propto$
Diff.	$J_{im} = 0, \quad x_s \to \infty, \quad d \to 0$	$-1/r_i$	$-t^{2/3}$
At/Det	$J_{im} = 0, \quad x_s \to \infty, \quad d \to \infty$	$1 - \frac{r_i}{R}$	$-t$
Growth	$x_s \to \infty, J_{im}\tau > n_{eq}$	r_i	t^2
Sublim.	$x_s \to \infty, J_{im}\tau > n_{eq}, r_i = R$	$-r_i$	$-t^2$

Table 1: *Asymptotic scaling laws for different mechanisms (limited by diffusion, limited by attachment/detachment, pure growth or pure sublimation). The last column has been obtained by writting for a circular island $dA/dt = 2\pi r_i dr_i/dt$.*

We report in the following figures various plots of dA/dt versus r_i. All the following figures have been calculated with $R = 2$ and $0 < r_i < 1$. In this case we consider that R variations (that are not considered in the analytical model) do not affect significantly r_i variations.

Figures 10a, b, c report the evolution of dA/dt versus r_i for decreasing values of x_s (that means for increasing sublimation) in absence of any external flux ($J_{in} = 0$) calculated in the diffusion-limited case ($d \to 0$). Figure 10d shows a similar trend in the attachment/detachment limited case ($d \to \infty$). In the diffusion limited case, the asymptotic behaviours agree with those reported in table 1: they show that in absence of sublimation ($x_s \to \infty$) $dA/dt \to -1/r_i$ whereas for strong sublimation ($x_s \to 0$) $dA/dt \to -kr_i$. Also, in the attachment/detachment limited case, $dA/dt \to -k$ in absence of sublimation ($x_s \to \infty$) but there is still $\to -kr_i$ for strong sublimation ($x_s \to 0$).

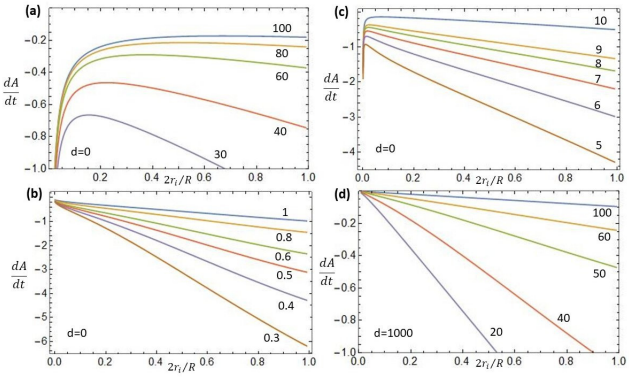

Figure 10: *dA/dt (arbitrary units) versus r_i: Diffusion limited ($d \to 0$), x_s varying between 100 and 30 (a) , between 1 and 0.3 (b) and between 10 and 5. In absence of sublimation ($x_s \to \infty$) $dA/dt \to -1/r_i$ whereas for strong sublimation $x_s \to 0$ $dA/dt \to -kr_i$. (d) For attachment detachment limited ($d \to \infty$) $dA/dt \to -k$ in absence of sublimation but $\to -kr_i$ for strong sublimation. (The external radius has been fixed to $R = 2$. The vertical axis has been multiplied by 10^4, 10^3,10^1 and 10^4 respectively for a, c, b and d graphs respectively).*

Figure 11 shows dA/dt as a function of r_i in presence of an impinging flux $J_{im} > 0$. For the diffusion limited case ($d \to 0$, Figure 11a) the initial curve $dA/dt \to -1/r_i$ valid for $J_{im} = 0$ becomes $dA/dt \to +kr_i$ whereas for the attachment/detachment limited case ($d \to \infty$) the curve $dA/dt \to -kr_i$ valid for strong sublimation (weak values of x_s) becomes $dA/dt \to +kr_i$ in presence of high enough external flux as expected.

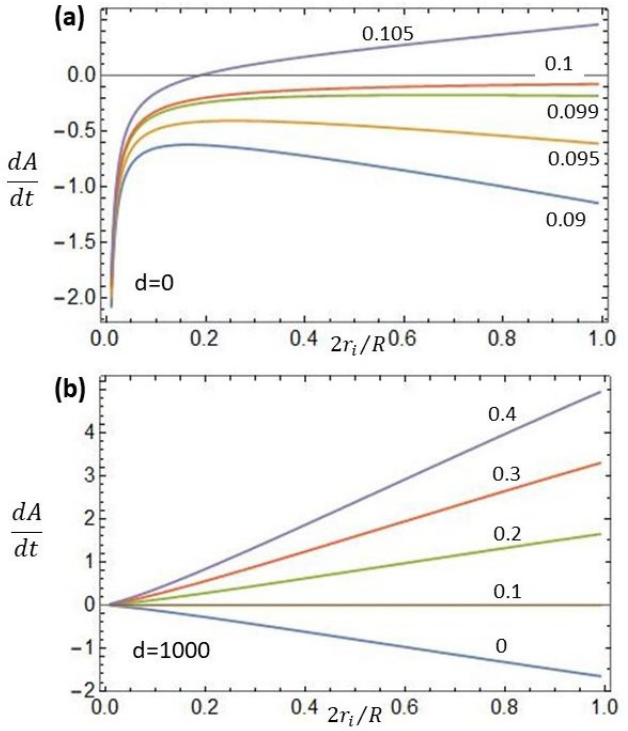

Figure 11: *Flux effect on dA/dt (arbitrary units) versus x: (a) diffusion limited ($d \to 0$ and $x_s = 10$) $J_{im}\tau$ varying between 0.09 and 0.105. and (b) Attachment/Detachment limited ($d \to \infty$ and $x_s = 10$) with $J_{im}\tau$ varying between 0 and 0.4. Vertical axis are given in 10^{-4} units*

The graphs of Figures 10 and 11 thus confirm the asymptotic scaling laws and explain the results of the KMC simulations. However the analytical results are only valid for $R >> r_i$ and thus do not really allow to discuss geometrical effects as the difference between wedding cake and island-in-a-hole.

3.2. Is it possible to balance the desorption ?

Let us now consider the simpler case of a terrace framed by two steps. Figure 12a shows the number of atoms versus time, extracted from KMC simulation, for a bare surface with two steps (green triangles) and for a 2D island between two steps (red circles). The slope of the line passing through the red circles is larger than that passing through the green triangles. This means that the presence of the 2D island of radius r_i increases the number of sublimating atoms with respect to the bare terrace since additional atoms detach from the island edge.

The effect of an impinging flux in simulations with an island between two steps is shown in Figures 12b and c. Figure 12b shows the total number of atoms as a function of time for a 2D island between two steps with an impinging flux adjusted to stop the step motion that exists in absence of the 2D island. In these conditions, the total number of atoms decreases as long as the island exists. Only when the island disappears the number of atoms becomes then remains constant.

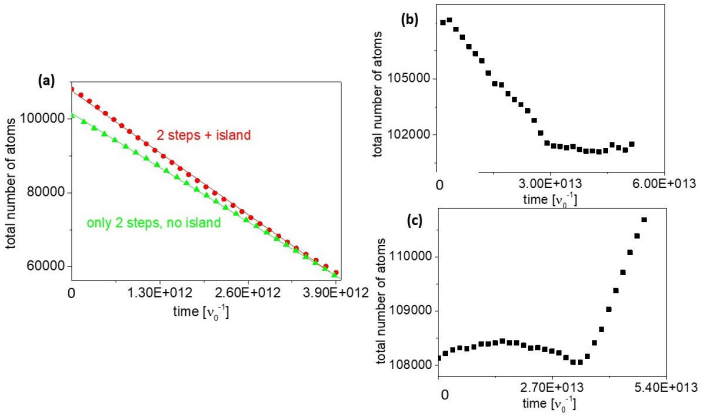

Figure 12: *(a) Number of atoms on the surface for a bare surface with two steps (green triangles) and an island between two steps (red circles). The sublimation flux of the bare surface is obtained from the slope of the green curve, (b) Effect of an impinging flux equal to the sublimation flux of the bare surface: the number of atoms reaches a constant value only after complete disapperance of the circular island. (c) Effect of an impinging flux slightly larger than the sublimation flux: the step motion engulfes the island. (k_BT=0.25 J, $R = 250$, $r_i = 45$, $\ell = 375$Simulation box 600x600). The impinging flux in (b) is 1 atom every $4\,10^6\,\nu_o^{-1}$, in (c) it is $3.83\,10^6\,\nu_o^{-1}$.*

Figure 12c shows the number of atoms versus time for an impinging flux slightly larger than the flux used in Figure 12b. At the beginning the total number of atoms increases because the island curvature is large and its edges behave almost like straight steps that supply adatoms. Then, because of the Gibbs-Thomson effect, the island shrinks so that its perimeter supplies less adatoms to the surface. When the island has disapperared the linear increase simply corresponds to the step motion induced by step incorporation of the additional impinging atoms[3].

Results are similar for an island in a hole or for the wedding cake configuration: the presence of a 2D island modifies the adatom concentration and thus makes impossible to properly define a steady state situation.

More generally, the system (island + steps) can never be stabilized by an external flux because whatever the conditions (with or without sublimation), the island tends to disappear or the steps advance and incorporate the island.

4. Discussion and conclusion

Let us consider the possible compensation of the sublimation by an additional impinging flux as described in Figure 1. In case of a vicinal surface it is perfectly possible to exactly compensate the sublimation by a constant additional flux since a vicinal surface may correspond to an equilibrium situation[4].

[3] Notice that it should be possible to choose a higher value of the additional flux that should stabilize the 2D island (no more shrinking), however in this case the steps advance then engulfe the 2D island which again disappears.

[4] A crystal can have various facets but in equilibrium with a vapour.

This is not the case for 2D islands on a surface since their situation never corresponds to an equilibrium state (see subsection 3.2). In KMC simulations it is possible to exactly compensate at each time the desorbing flux with a deposition flux but, due to the island shrinking, this flux must vary with the island perimeter and thus with time. In experiments (Figure 1) it is far from trivial to adjust in real time the deposition flux.

A first remark thus is that the experimental configuration depicted in Figure 1a does not generally force the system to be in equilibrium.

Let us now consider the dynamic evolution of 2D islands on a surface. Generally, the area of a 2D island may be fitted by a power law $A(t) \propto (t_0 - t)^{\alpha}$. The exponent α depends on the mechanism at work but also on the experimental conditions (geometrical configurations and existing fluxes). In absence of sublimation and external flux, $\alpha \to 2/3$ in the diffusion-limited regime and $\alpha \to 1$ in the attachment/detachment regime. When, in the diffusion limited regime, sublimation is supplemented by an external flux the exponent α increases from 2/3 (zero external flux) towards 2 (pure growth) and thus passes through unity for a specific value of the flux. Such a variation thus cannot be interpreted by a transition from a diffusion-limited regime towards an attachment/detachment regime. Our KMC simulations confirm the prediction of the analytical expressions and the exponents α approach the asymptotic values (0.78 close to 2/3, 1.72 close to 2 and 0.9 close to 1). KMC simulations also evidence some geometrical effects, as for instance, the difference of behaviour between an island in a hole and a wedding cake configuration.

A second remark is thus that the value of the exponent α in the scaling law $A(t) \propto (t_0 - t)^{\alpha}$ is not enough to identify the mechanism at work, at least in presence of sublimation and impinging fluxes.

Several possible effects have not been considered in these simplified approaches. For instance one might wonder about the effect of specific edge properties as step transparency [3], Ehrlich-Schwoebel barrier [25] or deviations from Gibbs Thomson equations that could exist for small islands and high vapour densities [13]. Following Ref [3], edge transparency change is generally due to non-equilibrium steps present at low temperature and thus should not play in the high temperature range we have considered. The Ehrlich-Schwoebel barrier introduces two new kinetic lengths d^+ and d^- (for up and down hops) that can be usually merged in an effective kinetic length [10] and thus should not modify the asymptotic scaling laws. Last but no least, deviations from the classical Gibbs-Thomson effect only occur for very small islands [13] beneath the size usually studied in experiments. In our analytical calculations we have neglected the effect of advacancies that could play a role especially when sublimation takes place. However, on the basis of ref [26] the effect of ad-vacancies should not modify asymptotic laws as confirmed by our KMC simulations (where advacancies exist).

To conclude, our work provides a basis for further experiments, in particular for studying the evolution of experimental scaling laws far from the classical case (no sublimation nor impinging flux). Beyond these fundamental considerations, the study of the effect of an external flux on the surface dynamics could be important in a few industrial processes in which Si wafers are stacked at high temperature and thus exposed to fluxes generated by each other [8].

Appendix I KMC model

KMC simulations have been used to complete the analytical approach of the area evolution of 2D circular islands. Indeed, KMC simulations (i) enable to relax the strong assumptions used to obtain asymptotic analytical expressions, (ii) take into account the edge fluctuation of both r_i and R.

In our KMC model [27] the atoms jump from a position to a nearest neighbor empty position, in a 3D face centered cubic lattice (fcc). The island surface corresponds to a (111) plane of a fcc crystal. Atoms of the first layer are in contact with a frozen layer underneath. The distance between two nearest neighbor positions is the lattice unit, that we take equal to 1. Atoms jump with a rate equal to $\nu_0 \exp[-nJ/(k_B T)]$, where n is the number of nearest neighbors (for instance, for an adatom $n = 3$ because of the three neighbors in the layer under the adatom), J is a bond energy, taken as the energy unit in our system, k_B is the Boltzmann constant and T is the temperature. The attempt frequency ν_0 is taken equal to 1 for all atoms. In simulations with sublimation, atoms can also sublimate, i.e. can be removed from the simulation, if they have less than 12 neighbors. Similarly to atomic jumps, the sublimation rate is equal to $\nu_0 \exp[-(nJ + E_{ev})/(k_B T)]$, where E_{ev} is an sublimation energy that we have typically taken between 0 and 4 J. To simulate a deposition that compensates sublimation, when an atom sublimates, it is not removed from the simulation, but it is put in a random position on the surface. In some simulations (see Figure 12) deposition does not compensate sublimation, but sublimating atoms are removed and atoms are added in a random position on the surface at definned time intervals. At each move (atomic jump, sublimation or sublimation/deposition) the time advances by the inverse of the sum of all jump rates and can thus be expressed in units ν_0^{-1}.

Appendix II Analytical model

Let us consider a circular island of radius r_i inside a larger circular hole of radius R. In such conditions, following references [15, 16] the adatom concentration is obtained by solving equation 1 in circular coordinates *id est* with $\nabla^2 n = \frac{\partial^2 n}{\partial r^2} + \frac{1}{r}\frac{\partial n}{\partial r}$.

The general solution is

$$n(r) = B_I I_0(r/x_s) + B_K K_0(r/x_s) + J_{im}\tau \qquad (4)$$

where $I_n(r)$ and $K_n(r)$ are the n^{th} order modified Bessel functions of the first and second kind respectively and B_I and B_K two constants that can be determined from the following boundaries conditions that describe the net flux that detach from the inner island towards the surrounding step (for impermeable edges)

$$-D\frac{dn}{dr}\Big]_{r_i} = \kappa\left(n_{eq}(r_i) - n(r_i)\right) \tag{5}$$

$$-D\frac{dn}{dr}\Big]_{R} = -\kappa\left(n_{eq}(R) - n(R)\right) \tag{6}$$

where κ is a kinetic coefficient and $n_{eq}(r)$ the adatom concentration at equilibrium.

We thus obtain

$$B_I = \frac{D_K\left(\theta_{eq}(R/x_s) - J_{im}\tau\right) + C_K\left(\theta_{eq}(r_i/x_s) - J_{im}\tau\right)}{D_K C_I + C_K D_I} \tag{7}$$

$$B_K = \frac{D_I\left(\theta_{eq}(R/x_s) - J_{im}\tau\right) - C_I\left(\theta_{eq}(r_i/x_s) - J_{im}\tau\right)}{D_K C_I + C_K D_I} \tag{8}$$

with

$$\begin{cases} C_K = K_0\left(R/x_s\right) - \left(\frac{d}{x_s}\right) K_1\left(R/x_s\right) \\ C_I = I_0\left(R/x_s\right) + \left(\frac{d}{x_s}\right) I_1\left(R/x_s\right) \\ D_K = -K_0\left(r_i/x_s\right) - \left(\frac{d}{x_s}\right) K_1\left(r_i/x_s\right) \\ D_I = I_0\left(r_i/x_s\right) - \left(\frac{d}{x_s}\right) I_1\left(r_i/x_s\right) \end{cases} \tag{9}$$

where $d = D/\kappa$ is the so-called kinetic length.

The rate at which the island area A changes by diffusion towards the surrounding step is given by $\frac{dA_1}{dt} = -2\pi r_i \Omega j_{net}$ where $j_{net} = \kappa\left[n_{eq}(r_i) - n(r_i)\right]$

Putting altogether we find

$$\begin{aligned} \frac{dA_1}{dt} = &-\frac{2\pi D\Omega}{D_K C_I + C_K D_I}.\widetilde{r_i} \\ &\{n_{eq}(R).\left[D_I K_1(\widetilde{r_i}) - D_K I_1(\widetilde{r_i})\right] \\ &-n_{eq}(r_i).\left[C_K I_1(\widetilde{r_i}) + C_I K_1(\widetilde{r_i})\right] \\ &+J_{im}\tau.\left[\left(C_K + D_K\right) I_1(\widetilde{r_i}) + \left(C_I - D_I\right) K_1(\widetilde{r_i})\right]\} \end{aligned} \tag{10}$$

Which is the area change due to the adatom flux from the inner island towards the outer step.

However adatoms may also detach from the island edge then diffuse on the island itself before being desorbed.

This supplementary contribution to the area change may be calculated by solving the equation 1 whose solution simply reads $n(r) = \mathcal{B}_I I_0(r/x_s) + J_{im}\tau$ to avoid the divergence of $K_0(r_i{=}0)$ that should appear with the solution given in equation 4.

The boundary conditions coefficient $\mathcal{B}_I$ can be found via the boundary condition

$$-D\frac{dn}{dr}\Big]_{\pm r_i} = \mp\kappa\left(n_{eq}(\pm r_i) - n(\pm r_i)\right) \tag{11}$$

with $n_{eq}(r_i) = n_{eq}(-r_i)$ and $n(r) = n(-r_i)$. We thus find

$$\mathcal{B}_I = \frac{n_{eq}(r_i) - J_{im}\tau}{I_0(\widetilde{r_i}) + \frac{d}{x_s} I_1(\widetilde{r_i})} \tag{12}$$

The net flux now is $j_2 = -D\frac{dn}{dr}\Big]_{r_i}$ so that equation $\frac{dA_2}{dt} = -2\pi r_i \Omega j_2$ gives the contribution

$$\frac{dA_2}{dt} = -2\pi D\Omega\widetilde{r_i}\frac{\left(n_{eq}(r_i) - J_{im}\tau\right)}{I_0(\widetilde{r_i}) + \frac{d}{x_s} I_1(\widetilde{r_i})} \tag{13}$$

The total change of area thus reads:

$$\frac{dA}{dt} = \frac{dA_1}{dt} + \frac{dA_2}{dt} \tag{14}$$

where dA_1/dt and dA_2/dt are given by equations 10 and 13.

When using the Gibbs Thomson relation, the equilibrium concentration at the island boundary reads

$$n_{eq}(r) = n_{eq}\exp\left(\frac{\beta\Omega}{r k_B T}\right) \tag{15}$$

where β is the edge energy per unit length of inner and outer islands.

Notice that in this description a wedding-cake configuration (2D island sit on a 2D island) simply differs form a 2D island-in-a-hole configuration by the sign of the radius R (positive or negative for island and hole respectively).

In absence of any impinging flux $J_{im} = 0$) and without sublimation ($x_s = 0$), one recovers the classical expression [13, 15, 16, 28] :

$$\frac{dA}{dt} = -2\pi D a^2 n_{eq}\frac{e^{\beta\Omega/r_i k_B T} - e^{\beta\Omega/R k_B T}}{ln\left|\frac{r_i}{R}\right| + \frac{d}{r_i}} \tag{16}$$

This last expression may be simplified using the approximation $\exp\left(\frac{\beta\Omega}{r k_B T}\right) \simeq \left(1 + \frac{\beta\Omega}{r k_B T}\right)$ valid for $\frac{\beta\Omega}{r k_B T} << 1$ so that

$$\frac{dA}{dt} = -2\pi D a^2 n_{eq}\frac{\beta\Omega}{k_B T}\frac{\frac{1}{r_i} - \frac{1}{R}}{ln\left|\frac{r_i}{R}\right| + \frac{d}{r_i}}$$

With this condition, two asymptotic cases naturally arise [13, 15, 28]: (i) the Diffusion Limited (DL) regime when $d \to 0$, which leads to $A(t) \propto t^{2/3}$ and the (ii) Attachment-Detachment (AD) regime when $d \to \infty$ (actually $d >> r_0 ln\left|\frac{r_o}{R}\right|$) that leads to $A(t) \propto t$. Notice that for large R, dA/dt no more depends on R so that wedding-cake ($R > 0$) and island in a hole ($R < 0$) lead to similar results.

The existence of such asymptotic laws helps to identify the leading mechanism in experiments (DL or AD) by measuring the exponent α in the experimentally recorded scaling law $A(t) \propto (t_0 - t)^{\alpha}$.

When the two fluxes J_{in} and J_{des} exist, the solution of equation 14 is much more complex than equation 16. Using more drastic approximations enables to recover classical scaling laws (see table 1 in the main

text)

	$\frac{1}{n_{eq}}\frac{dA}{dt}$
$x_s \to \infty$	$\frac{(\exp(\xi/R)-\exp(\xi/r_i))}{\ln(R/r_i)+d(1/R+1/r_i)}$
$d \to 0$ $x_s >> R, r_i$	$\frac{(\exp(\xi/R)-\exp(\xi/r_i))}{\ln(R/r_i)}\left(1-\frac{1}{4}(\widetilde{r_i})^2\right)$
$d \to 0$ $\widetilde{r} = r_i/x_s$	$\frac{r_i}{x_s}\frac{\left[I_0(\widetilde{R})\exp(\xi/R)-I_0(\widetilde{r_i})\exp(\xi/r_i\right]\left[I_1(\widetilde{r_i})K_0(\widetilde{r_i})+I_0(\widetilde{r_i})K_1(\widetilde{r_i})\right]}{I_0(\widetilde{r_i})\left[I_1(\widetilde{r_i})K_0(\widetilde{R})-I_0(\widetilde{R})K_0(\widetilde{r_i})\right]}$

Table 2: *A few asymptotic behaviors obtained for $J_{im} = 0$ with $\xi = \frac{\beta\Omega}{kT}$ the capillary length and $\widetilde{r} \equiv r/x_s$. Let us recall that since $dA/dt = 2\pi r_i dr_i/dt$ asymptotic expressions of $A(t)$ may be obtained (see table 1).*

References

[1] H. Bethge, K. Keller, E. Ziegler, Journal of Crystal Growth 3 (1968) 184.

[2] W. Burton, N. Cabrera, F. Frank, Phil. Trans. Roy. Soc. A 243 (1951) 299.

[3] S. Filimonov, Y. Hervieu, Surf. Sci. 553 (2004) 133.

[4] J. Métois, J. Heyraud, A. Pimpinelli, Surf. Sci. 420 (1999) 250.

[5] O. Pierre-Louis, J. Métois, Phys. Rev. Lett. 93 (2004) 165901.

[6] J. Métois, P. Müller, Surf. Sci. 548 (2004) 13–21.

[7] B. Ranguelov, J. Métois, P. Müller, Surf. Sci. 600 (2006) 4848–4854.

[8] S. Lachman-Shalem, N. Shafry, I. Rabinovitch, R. Mor, M. Wolovelsky, D. H. Z. Neidik, Proceedings of spie, in: M. M. K. Ashtiani (Ed.), Process Control and Diagnosis, volume 4182, SPIE, 2000, p. 242.

[9] W. Burton, N. Cabrera, F. Frank, Philos. Trans. R. Soc. London A 243 (1951) 299.

[10] A. Pimpinelli, J. Villain, Physics of crystal growth, Cambridge University Press, 1997.

[11] B. Mutaftschiev, The atomistic nature of crystal growth, in: C. Godreche (Ed.), Current Topics in Mat. Sci., Springer, 2001, p. 1.

[12] D. Peale, B. Cooper, J. Vac. Sci. Tech. A. 10 (1992) 2210.

[13] B. Krishnamachari, J. Lean, B. Cooper, J. Sethna, Phys. Rev. B. 54 (1996) 8899.

[14] K. Morgenstern, G. Rosenfeld, G. Comsa, Phys. Rev. Lett. 76 (1996) 2113.

[15] M. Giesen, Prog. Surf. Sci. 68 (2001) 1.

[16] A. Pang, K. Man, M. Altman, T. Stasevitch, F. Szalma, T. Einstein, Phys. Rev. B. 77 (2008) 115424.

[17] J. P. de Boer, I. Ford, L. Kantorovitch, D. Vvedensky, J. of Chem. Phys. 149 (2018) 194107.

[18] C. Sprodovski, K. Morgenstern, Phys. Rev. B. 100 (2019) 045402.

[19] P. Spurgeon, K. Lai, J. Evans, P. Thiel, J. Phys. Chem. C; 124 (2020) 7492.

[20] J. Gibbs, On the equilibrium of heterogenous substances, Transactions of the Connecticut Academmy of Arts and Sciences, 1878.

[21] J. Thomson, Application of dynamics to Physics and Chemistry, London, Macmilan et Co, 1888.

[22] J. Métois, P. Müller, J. Heyraud, Surf. Sci. 446 (2000) 187.

[23] K. Man, W. Tang, X. Jin, M. Altman, Surf. Interf. Analys. 38 (2006) 1632–1635.

[24] F. Leroy, D. Karashanova, M. Dufay, J. Debierre, T. Frisch, J. Métois, P. Müller, Surf. Sci. 603 (2009) 507.

[25] A. Saul, J. Métois, A. Ranguis, Phys. Rev. B. 65 (2002) 075409.

[26] A. Pimpinelli, J. Villain, Physica A. 204 (1994) 521.

[27] S. Curiotto, P. Müller, F. Cheynis, F. Leroy, Appl. Surf. Sci. 552 (2021) 149454.

[28] G. Icking-Konert, M. Giesen, H. Ibach, Surf. Sci. 398 (1998) 37–48.